

Article

# Synthesis and Characterization of a New Aluminosilicate Molecular Sieve from Aluminosilica Perhydrate Hydrogel

Haiqiang Ma <sup>1</sup>, Kun Jiao <sup>2</sup>, Xiangyu Xu <sup>1</sup> and Jiaqing Song <sup>1,\*</sup>

<sup>1</sup> State Key Laboratory of Chemical Resource Engineering, Beijing University of Chemical Technology, Beijing 100029, China; 18101218769@163.com (H.M.); xuxy@mail.buct.edu.cn (X.X.)

<sup>2</sup> College of Chemistry and Molecular Engineering, Peking University, Beijing 100871, China; lovelyjjq0809@163.com

\* Correspondence: songjq@mail.buct.edu.cn

Received: 6 October 2020; Accepted: 26 November 2020; Published: 30 November 2020



**Abstract:** A novel structure aluminosilicate molecular sieve, named BUCT-3, was prepared by dynamic hydrothermal synthesis, and the critical factor to obtain the new structure is using an active silicon and aluminum source, aluminosilica perhydrate hydrogel. Meanwhile, only high content of O-O bonds can ensure the pure phase of BUCT-3. Through the characterization of x-ray powder diffraction (XRD), Fourier transform infrared spectra (FTIR), scanning electron microscopy (SEM), and so on, some structure and morphology information of BUCT-3 molecular sieves as well as the special silicon and aluminum source was obtained. It's worth noticing that the O-O bonds of reactants can be reserved in the products, and thus, help us to get a new structure with cell parameters  $a = 8.9645 \text{ \AA}$ ,  $b = 15.2727 \text{ \AA}$ ,  $c = 11.3907 \text{ \AA}$ ,  $\alpha = 90^\circ$ ,  $\beta = 93.858^\circ$ ,  $\gamma = 90^\circ$ . The crystal system is monoclinic. Though the thermostability of BUCT-3 is not satisfactory, its potential application derived from O-O bonds cannot be neglected.

**Keywords:** aluminosilica perhydrate hydrogel; molecular sieve; peroxides; silicon-aluminum source; synthesis method

## 1. Introduction

Zeolites are microporous crystalline inorganic materials with well-defined pore systems. Since the 1940s, the study of zeolites with new structure has attracted a great deal of interest for their specific catalytic or adsorption properties [1,2]. Much effort has been devoted to developing novel molecular sieves [3,4].

Generally speaking, molecular sieves with new structures can be obtained in three ways: (i) Zeolites synthesized by using structure-tunable organic ammonium salt template: This method usually requires the use of organic amine/ammonium cations as structure directing agents (SDAs). Although designing new structures of templates is expected to be the most useful way to synthesize new structural molecular sieves, it's also the most complicated method [5–7]. (ii) Molecular sieves synthesized by using heteroatom substitution [8]: heteroatom molecular sieves using other elements, such as Ti, Cr, Zr, and Ga [9–11], partially substitute silicon, aluminum, or phosphorus in the framework to form heteroatom-containing molecular sieves. These elements that enter the framework can be main group elements, or transition elements from 2+ to 5+. Due to the introduction of specific non-metal or metal atoms, many new molecular sieves with special structures have been successfully synthesized. (iii) Molecular sieves synthesized by topotactic transformation [12,13]: two steps are required to obtain three-dimensional structure molecular sieves from two-dimensional layered precursors: (a) Preparation of layered precursors by traditional hydrothermal synthesis;

(b) the two-dimensional precursor undergoes interlayer dehydration and condensation through high-temperature solid-phase reaction to form a three-dimensional molecular sieve, which is the process of topological transformation [5].

Many parameters can also influence the crystallinity, morphology, and even structure of molecular sieves, such as SDA/ $\text{TO}_2$ ,  $\text{OH}^-/\text{TO}_2$ , and  $\text{H}_2\text{O}/\text{TO}_2$ , as well as the synthesis temperature, crystallization time, and so on [14].

Another important feature of molecular sieves synthesis is that even if the other conditions of crystallization are the same, different framework structures may be obtained if different sources of reactants are used, especially the essential element of structure. It is known that the use of different silica sources may affect the type of zeolites [15–17], crystal size [17–25], morphology [20,21,25], and the rate of crystallization [15,16,19–24], since the fragile silicate intermediates releasing during the process of the silica dissolution plays an important role in the framework formation [26]. A typical example [27] is that scientists from Union Carbide Corporation converted an inert silicon-aluminum source into an active source, and synthesized a series of new molecular sieves ranging from A to Y, indicating that the activity of the source affects the structure of the molecular sieve. This work has inspired us to synthesize new molecular sieves by changing the activity of raw materials.

Hydrogen peroxide is a clean and green chemical product. Its special electronic structure enables it to increase the activity of some reactions. Compared with the design of complex, expensive, and polluting organic templates to synthesize new molecular sieves, relatively inexpensive hydrogen peroxide is used to treat the reaction raw materials in order to change the activity of the source, so as to carry out the reaction process with low energy consumption. Considering cost-effectiveness and environmental cleanliness, it is advantageous to change the synthesis method of raw material activity to obtain new molecular sieves.

In this article, a new kind of aluminosilicate molecular sieve with novel structure was obtained by using a usual template, tetrapropylammonium hydroxide (TPAOH) as the SDA, and unusual reactants, aluminosilica perhydrate hydrogel as the silicon and aluminum source. This is an unstable structure with peroxide bond that makes the structure elucidation very difficult. However, a combination of x-ray powder diffraction (XRD) and Fourier transform infrared spectra (FTIR) gives some partial structure of the novel material. We also explored in detail the effects of different silicon and aluminum sources, temperatures, and time on the products.

## 2. Materials and Methods

### 2.1. Chemicals

The chemicals used in our study were as following: tetraethoxysilane (TEOS, 28 wt%  $\text{SiO}_2$ , Guang Dong Fine Chemicals Co., Ltd., Guangdong, China), tetrapropylammonium hydroxide (TPAOH 25 wt% in water, Shanghai Aladdin Bio-Chem Technology Co., LTD, Shanghai, China), Ammonia solution ( $\text{NH}_3$  25–28 wt%, Beijing Chemical works Co., Ltd., Beijing, China), hydrogen peroxide ( $\text{H}_2\text{O}_2$  30 wt%, Beijing Chemical works Co., Ltd., Beijing, China) and deionized water, sodium aluminate ( $\text{Al}_2\text{O}_3$  50–56 wt%,  $\text{Na}_2\text{O}$  40–45 wt%, Fisher, UK), and sodium silicate ( $\text{Na}_2\text{SiO}_3$ , Guang Dong Fine Chemicals Co., Ltd., Guangdong, China).

### 2.2. Synthesis

**Silica gel:** A certain amount of ammonium fluoride was dissolved in deionized water according to the molar ratio of 0.004:4 to obtain solution A. Then, solution A was added dropwise to Solution B consisting of ethanol, water, and TEOS in a molar ratio of 8:4:1. After stirring until uniform, a transparent gel is obtained, which is dried in an oven at 50 °C for 1 d, and then roughly ground after taking it out. Finally, it is calcined in a muffle furnace at 800 °C for 2 h.

**Aluminosilica perhydrate hydrogel-1 (SiAl-1):** Aluminosilica perhydrate hydrogel-1 was prepared by dissolving a fixed amount of  $\text{NaAlO}_2$  and  $\text{Na}_2\text{SiO}_3$  ( $\text{Si}/\text{Al} = 25$ ) in deionized water, and then  $\text{H}_2\text{O}_2$

were added dropwise to the above solution and stirred for 1 h at room temperature. After drying at 50 °C for 24 h, the product was named as SiAl-1. The initial feed ratio of the gel was:  $\text{Al}_2\text{O}_3:\text{SiO}_2:\text{H}_2\text{O}_2:\text{H}_2\text{O} = 1:50:194:2162$ .

Aluminosilica perhydrate hydrogel-2 (SiAl-2): TEOS was dissolved in the mixture of ethanol and deionized water, followed by a small amount of ammonia solution to promote the hydrolysis process. Subsequently,  $\text{NaAlO}_2$  solution was added to the silica gel with fixed Si/Al ratio 25. After stirring for a few minutes,  $\text{H}_2\text{O}_2$  was then added dropwise to the mixture with continuous stirring at room temperature for 0.5 h. After drying at 50 °C for 24 h, the product was named as SiAl-2. The initial feed ratio of the gel was:  $\text{Al}_2\text{O}_3:\text{SiO}_2:\text{H}_2\text{O}_2:\text{H}_2\text{O} = 1:50:365:1720$ .

Preparation of aluminosilicate molecular sieves: All samples were prepared by dynamic hydrothermal synthesis. The mixture of TPAOH, silica source, aluminum source, and deionized water was directly transferred into a teflon autoclave (25 mL capacity) with continuous stirring for at least 6 h. Finally, the autoclave was transferred to a homogeneous reactor at 70–120 °C for 2–4 days. Then, solid products were centrifuged, followed by repeatedly washing with deionized water and drying at 60 °C overnight. The initial feed ratio of the mixture was  $\text{Al}_2\text{O}_3:\text{SiO}_2:\text{TPAOH}:\text{H}_2\text{O} = 1:50:25:2500$ .

### 2.3. Characterizations

The X-ray diffraction (XRD) measurement was performed to obtain the phase information of the molecular sieve samples. The XRD data were collected by Ultima III diffractometer (Rigaku Corporation, Tokyo, Japan) with Cu K $\alpha$  radiation, the scanning range is from 5° to 50°, scanning 3 times at a rate of 10° min<sup>-1</sup>.

Scanning electron microscopy (SEM) images were performed using ZEISS SUPER55 scanning electron microscope (ZEISS, Jena, Germany). Its acceleration voltage is 3 kV, and the magnification is  $1 \times 10^3$ – $1 \times 10^6$ .

Infrared spectra (IR) were collected on a Vector 22 FTIR spectrometer (Bruker, Leipzig, Germany) to obtain some structural information of the new molecular sieve (400–5000 cm<sup>-1</sup>).

In-situ variable temperature X-ray diffraction data were collected on a modified Bruker D8 Advance diffractometer equipped with MRI high temperature attachment, a graphite monochromator and LynxEye detector (Bruker, Leipzig, Germany), using a Cu K $\alpha$  radiation source ( $\frac{1}{4}$  1.5418 Å) in Bragg-Brentano geometry, with a step width of 0.02° in the 2 $\theta$  range from 5° to 50°, and the keeping time was 2 s per step. The heating rate was 10 °C min<sup>-1</sup>, and the sample was equilibrated for 300 s prior to XRD data collection at a certain temperature.

Element analysis of products were characterized by elemental analysis (EA) using a Vario El elemental analyzer (elementar Analysensysteme GmbH, Hanau, Germany).

X-ray photoelectron spectroscopy (XPS) measurements conducted by AXIS Ultra DLD (Kratos, Manchester, UK) with Al K $\alpha$  radiation (149.94 W).

## 3. Results and Discussion

As mentioned in the introduction, different silica or aluminum sources strongly influence the nucleation and crystallization of zeolites. Our initial experimental idea was to study the effect on ZSM-5 by using different silicon and aluminum sources. Yet, considerable work has examined the influence of common silicon sources, like tetraethylorthosilicate (TEOS), fumed silica, and colloidal silica, sodium metasilicate [28]. For this reason, we carefully selected a special silicon source and aluminum source, aluminosilica perhydrate hydrogel, to investigate the influence on the structure of ZSM-5. At the same time, by adjusting the synthesis conditions, we hope to synthesize a molecular sieve with a new structure.

### 3.1. Characterization of Raw Materials

Prior studies [29,30] have reported methods for preparing silica-alumina gel but there are few reports on the preparation of aluminosilica perhydrate hydrogel. In fact, the preparation method of the

aluminosilica perhydrate hydrogel is similar with the silica-alumina gel, except that part of the water in the silica-alumina gel was replaced by hydrogen peroxide solution when the aluminosilica perhydrate hydrogel was prepared. Peralumina or persilica is a complexation of alumina and hydrogen-peroxide, which contain peroxide or hydroperoxide groups. In our experiment, two kinds of aluminosilica perhydrate hydrogel were obtained, namely SiAl-1 and SiAl-2, which differed in the silicon and aluminum source used in the process. Figure 1 shows the XRD of SiAl-1 and SiAl-2; the bulging peaks show a clear amorphous phase. Figure 2 shows SEM images of the silicon and aluminum source SiAl-1 and SiAl-2. The images of both materials demonstrate spherically shaped nanoparticles of 20–50 nm. Obviously, the sample of SiAl-2 is more uniform and dispersal. Owing to the hydrolysis rate of TEOS in water is slow, the reaction process is easy to control, and the prepared colloidal particles have the same size without agglomeration.

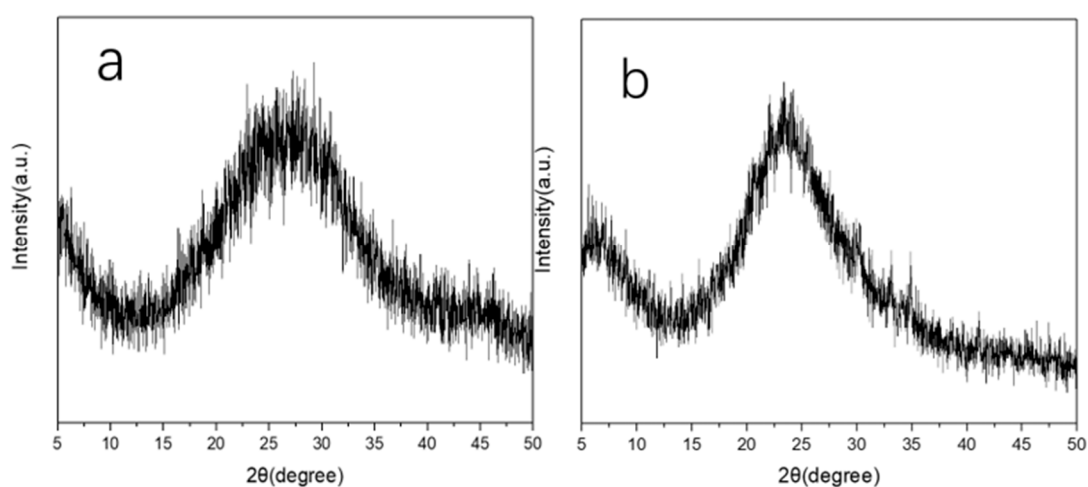


**Figure 1.** X-ray powder diffraction (XRD) patterns of sample (a) SiAl-1 and (b) SiAl-2.

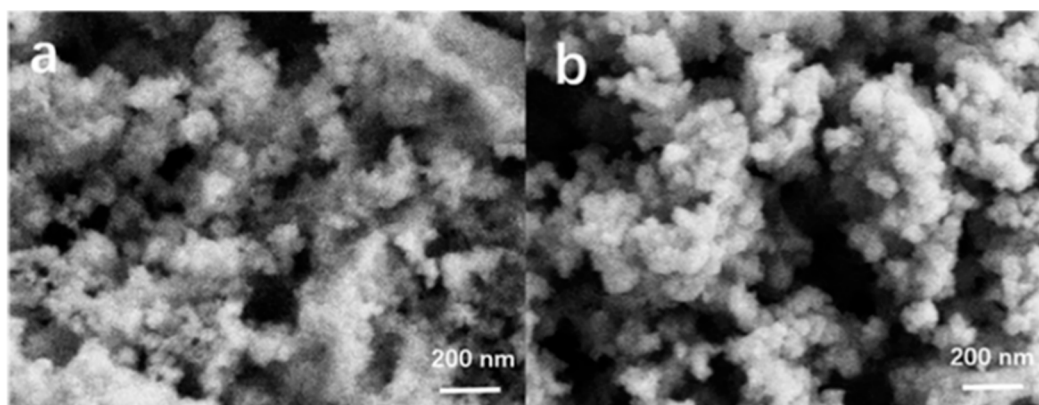


**Figure 2.** Scanning electron microscopy (SEM) images of sample (a) SiAl-1 and (b) SiAl-2.

The FTIR spectroscopy is an effective method for studying hydrogen peroxide complexes. Due to the unique electronic structure and geometric configuration of the hydrogen peroxide molecule, it can form a strong hydrogen bond with the hydroxyl group on the surface of the silica gel [31]. To confirm the O-O bonds were actually formed in the prepared aluminosilica perhydrate hydrogel, SiAl-1 and SiAl-2 sample was studied by the FTIR technique. Figure 3 shows the FTIR spectra of SiAl-1 and SiAl-2. The hydrogen bond formed by the O-H groups (Si-OH) with H<sub>2</sub>O and H<sub>2</sub>O<sub>2</sub> molecules was found to have a strong absorption peak near 3500 cm<sup>-1</sup>. However, the bending vibration of H-O-O (H<sub>2</sub>O<sub>2</sub>) connected to the silica framework was found to be weakly absorbed at

$1300\text{ cm}^{-1}$ . Previous studies [32,33] show that the sharp peak at  $876\text{ cm}^{-1}$  should be assigned to (O-O) stretching vibration of silica perhydrate, relatively speaking, the alumina perhydrate spectrum shows a broad peak here. Moreover, compared with SiAl-1, SiAl-2 has a relatively sharper peak, which means the concentration of O-O bond of SiAl-2 is higher than that of SiAl-1, since the sample/KBr ratio was fixed in all the FTIR analysis.

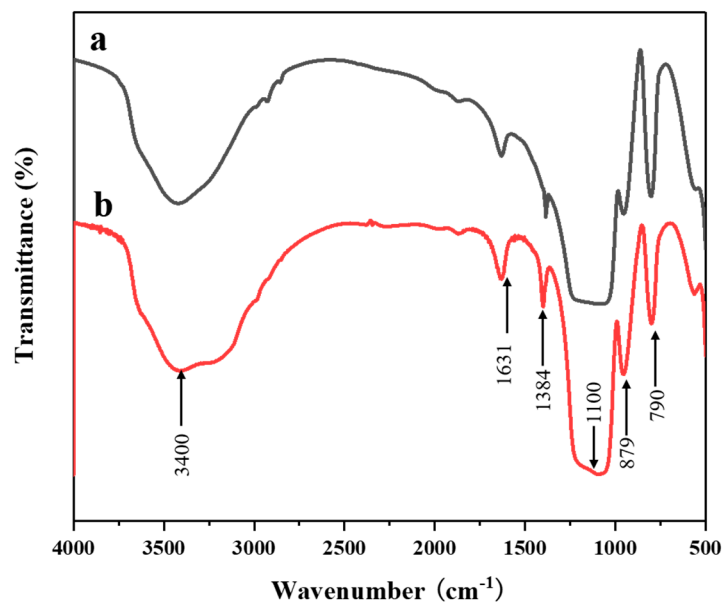


**Figure 3.** Fourier transform infrared spectra (FTIR) spectra of sample (a) SiAl-1 and (b) SiAl-2.

In order to study the species and relative content of oxygen in aluminosilica perhydrate hydrogel, high-resolution XPS spectra of O were used for peak fitting. Figure 4 shows XPS of sample (a) SiAl-1 and (b) SiAl-2. As can be seen from the figure, the spectra of SiAl-1 and SiAl-2 can be fitted into three components with peak positions of 530.1, 531.2, and 532.2 eV. According to previous research reports [34,35], the peak position of  $\text{O}_2^{2-}$  1s was found at 530 eV. The energy peak positions at 531 and 532 eV should correspond to the surface OH- and bulk T-O-T (T = Si, Al). At the same time, we have summarized the O 1s content of different species in SiAl-1 and SiAl-2 according to the quantitative calculation method of XPS, as shown in Table 1. It can be clearly seen from the table that the  $\text{O}_2^{2-}$  content in SiAl-2 is much higher than SiAl-2. This may be due to the preparation method of SiAl-2, that is, the continuous dropwise addition of hydrogen peroxide during the TEOS hydrolysis process can firmly lock the peroxide bond. This is completely consistent with the results of infrared analysis. Consequently, we successfully incorporated the O-O bond into the aluminosilica gel.

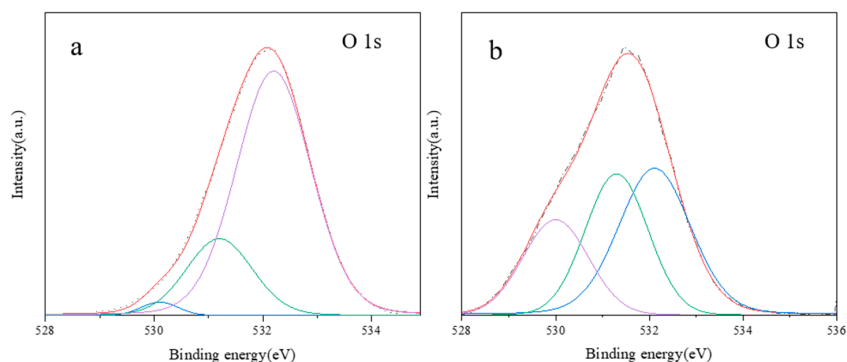


**Figure 4.** X-ray photoelectron spectroscopy (XPS) of sample (a) SiAl-1 and (b) SiAl-2.

**Table 1.** O 1s content of different species in SiAl-1 and SiAl-2 from XPS.

Sample	O <sub>2</sub> <sup>2-</sup> (%)	OH <sup>-</sup> (%)	Bulk O (%)
SiAl-1	2.1	21.6	76.1
SiAl-2	23.4	33.2	42.3

### 3.2. Optimized Synthesis and Characterization

ZSM-5 is a zeolite with MFI framework structure, usually prepared by hydrothermal synthesis, the reaction conditions were as follows: Al<sub>2</sub>O<sub>3</sub>:SiO<sub>2</sub>:TPAOH:H<sub>2</sub>O = 1:10–60:10–50:200–3000 at 100–175 °C for 1–8 days [36,37]. In our experiments, tetrapropylammonium hydroxide was chosen as the SDA. Two highly active aluminosilica perhydrate hydrogel were selected as the source. By contrast, silica gel and NaAlO<sub>2</sub> were selected as the common source of silica-aluminum. Since the silicon and aluminum source have peroxide groups, which have relatively high reactivity, the reaction should better be performed at a low temperature, like 90 °C. In order to intuitively express the synthesis conditions and results, we list the source, temperature, time, and phase in Table 2.

**Table 2.** The reaction conditions and the phases of Sample 1–9 (Al<sub>2</sub>O<sub>3</sub>:SiO<sub>2</sub>:TPAOH:H<sub>2</sub>O = 1:50:25:2500, 30 r/min).

Sample Number	Silicon and Aluminum Source	Temperature (°C)	Time (d)	Phase
Sample 1	SiO <sub>2</sub> + NaAlO <sub>2</sub>	70	4	amorphous
Sample 2	SiO <sub>2</sub> + NaAlO <sub>2</sub>	90	2	amorphous
Sample 3	SiO <sub>2</sub> + NaAlO <sub>2</sub>	90	4	amorphous
Sample 4	SiAl-1	70	4	NaP + BUCT-3
Sample 5	SiAl-1	90	2	NaP + BUCT-3
Sample 6	SiAl-1	90	4	NaP + BUCT-3
Sample 7	SiAl-2	70	4	BUCT-3 (L)
Sample 8	SiAl-2	90	2	BUCT-3
Sample 9	SiAl-2	90	4	BUCT-3

L: low crystallinity.

The SEM images of Sample 1–9 are shown in Figure 5. Notably, the morphologies of products obtained by using different silicon and aluminum sources are different. Thereinto, Samples 1–3 are nanosized particles, while Samples 4–6 are a mixture with two morphologies, including the spherical morphology and plate-like morphology. As for Samples 7–9, a plate-like morphology with lamellar structure is formed.

It can be seen from Figure 6 that except for the samples prepared with SiO<sub>2</sub> and NaAlO<sub>2</sub> as raw materials (Sample 1, 2, and 3) are amorphous, other samples have obvious characteristic peaks of BUCT-3 molecular sieve at  $2\theta = 9.68, 13.4,$  and  $24.78^\circ$ , whereas, the samples (Sample 4, 5, and 6) with SiAl-1 as source have characteristic peaks of NaP zeolite at  $2\theta = 12.51, 17.74, 21.71, 28.2,$  and  $33.5^\circ$ . However, no impurity peak (Sample 7, 8, and 9) was present in the XRD patterns when SiAl-2 was chosen as the starting source. Meanwhile, the crystallinity from Sample 7 to Sample 9 increased with increase of reacting time and temperature, which can be clearly seen from the height of peak at  $2\theta = 9.68^\circ$ .

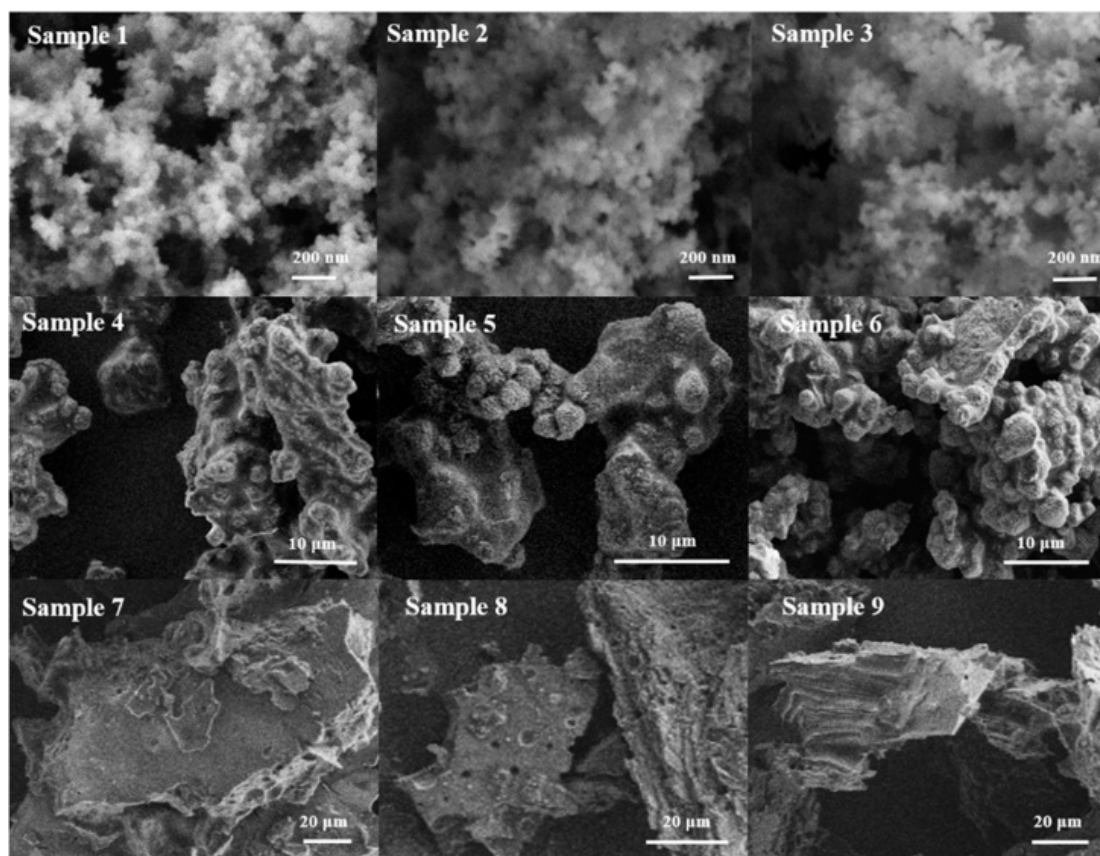


Figure 5. SEM images of Sample 1–9 with different reaction conditions.

As shown in Table 2, there are three kinds of phases in the products. In addition to the amorphous form, there are a known phase NaP zeolite, and a new phase of unknown structure, named BUCT-3. It's worth noticing that this new kind of molecular sieve can always be synthesized when the silicon and aluminum sources were treated with  $H_2O_2$  under all conditions. On the contrary, when common silicon and aluminum sources,  $SiO_2$  and  $NaAlO_2$ , were used in these conditions, the products were always amorphous. This implies that at this temperature, due to the low activity of ordinary source, the nucleation and growth of crystals are slower, and the final appearance is amorphous. Overall, these results are in excellent agreement with the SEM images observed. Undeniably, SiAl-1 and SiAl-2 with O-O bond formed by the addition of  $H_2O_2$  into the silica-alumina gel have higher reactivity. That is, the O-O bond plays a crucial role in the formation of the new molecular sieves.

It is well known that apart from crystallinity and morphology, the crystal phase is also affected by temperature. In order to further increase the crystallinity of BUCT-3, the temperature was raised to  $120\text{ }^\circ\text{C}$ ; the phase composition is shown in Table 3. Figure 7 shows the SEM images of Sample 10 and 11 prepared with different silica-alumina sources at  $120\text{ }^\circ\text{C}$ . It can be seen that both samples are sphere morphology packed with small particles, and the whole crystal size is about  $1\text{ }\mu\text{m}$ . Figure 8 shows the XRD patterns of both samples and they have typical MFI structure. It is clearly seen that further increase in temperature led to the appearance of ZSM-5 zeolites, which is contrary to our expectation. This is because that the O-O bond of SiAl-2 may break at the temperature  $120\text{ }^\circ\text{C}$ , and therefore, no O-O bond was involved in the reaction, which eventually led to the presence of ZSM-5. This result proves once again that the silica-alumina with O-O bond plays an important role in the formation of the structure of BUCT-3.

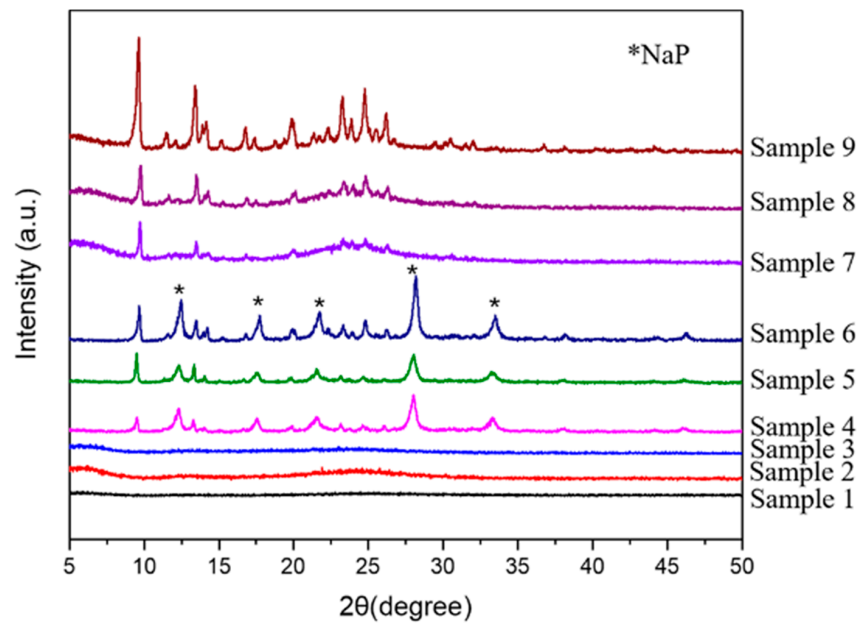


Figure 6. XRD patterns of Sample 1–9.

Table 3. The reaction conditions and phases of Samples 10 and 11.

Sample Number	Silicon and Aluminum Source	Temperature (°C)	Time(d)	Phase
Sample 10	SiO <sub>2</sub> + NaAlO <sub>2</sub>	120	2	ZSM-5
Sample 11	SiAl-2	120	2	ZSM-5

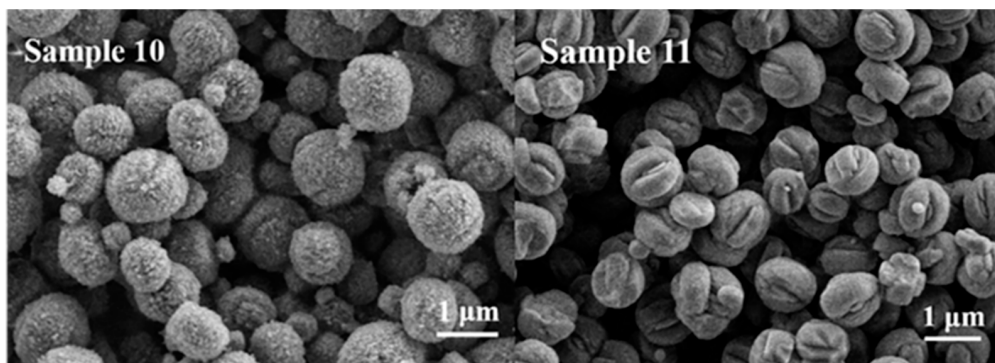
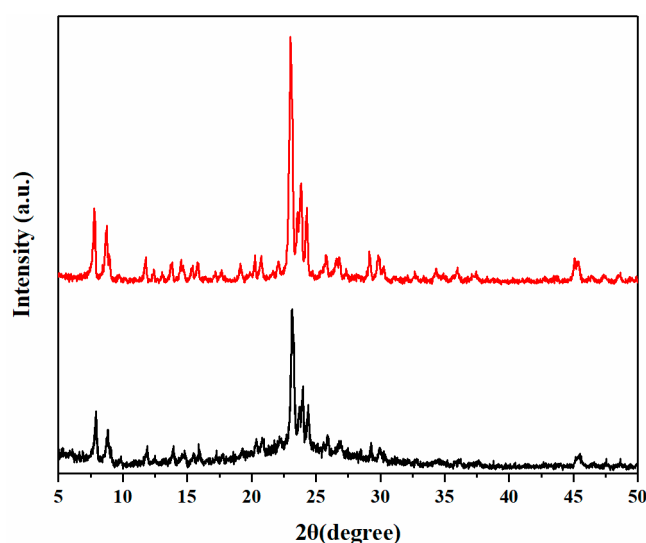


Figure 7. SEM images of Samples 10 and 11.



**Figure 8.** The XRD patterns of Samples 10 and 11.

### 3.3. Structural Analysis of BUCT-3 Molecular Sieves

Based on the discussion above, when SiAl-2 was chosen as the silicon and aluminum source and the reacting condition was set as 90 °C for 4 days, the product has the highest crystallinity. Therefore, Sample 9 was used to solve the structure of BUCT-3 molecular sieves.

The indexing of Powder X-ray Diffraction data of BUCT-3 was carried out by Fullprof program and the cell parameters are listed in Table 4. Since the result cannot match any known structure in the International Zeolite Association (IZA) database [38], that is, no structures' cell parameters have the same or multiple relationship with BUCT-3's, we can conclude that this is a new structure. Since the crystal size of the material cannot meet the conditions of single crystal diffraction, the crystal structure cannot be obtained from single crystal diffraction. Therefore, we consider using the selected area electron diffraction (SAED) method to analyze the sample, but the material is extremely intolerant to the electron beam and begins to melt within 2 min of irradiation (see Figure S1). The instability of materials brings many difficulties to the structural analysis.

**Table 4.** The unit cell parameters and crystal system of BUCT-3 molecular sieves by XRD.

Unit Cell Parameters	BUCT-3
a (Å)	8.9645
Standard deviation of a	0.0034
b (Å)	15.2727
Standard deviation of b	0.0067
c (Å)	11.3907
Standard deviation of c	0.0034
$\alpha$ (°)	90
$\beta$ (°)	93.858
$\gamma$ (°)	90
Crystal system	Monoclinic

Although the specific structure model of the BUCT-3 is not available, some structural information of the molecular sieve can still be obtained through FTIR, as shown in Figure 9. Based on the detailed study of the infrared bands of zeolite by the KSF [39], some characteristic infrared bands of silica-alumina molecular sieves were identified. The stretching vibration and bending modes of T-O-T (T = Si or Al) can be found to have strong absorption peaks at 424 cm<sup>-1</sup> and 970 cm<sup>-1</sup>, respectively. The symmetrical stretching vibration peak of the silicon (aluminum) oxygen tetrahedron inside the

framework can be found at  $650\text{--}750\text{ cm}^{-1}$ . Furthermore, there are typical stretching vibration bands of the SDA cation, tetrapropylammonium. The peaks near  $2992$  and  $2987\text{ cm}^{-1}$  are characteristic of C-H stretching vibration and the peaks near  $1483$  and  $1392\text{ cm}^{-1}$  are characteristic of N-C unsymmetrical bending vibration. Combined with the result of element analysis in Table 5, it is believed that the SDA cation was completely reserved in the framework, which means the structure directing property of TPA<sup>+</sup> was not destroyed by the O-O bonds of the reactants. As mentioned before, O-O stretching vibration can be found at the peak near  $873\text{ cm}^{-1}$ , and this can explain the poor thermostability of BUCT-3 molecular sieves. On the other hand, the existence of O-O bonds in the framework may help to form a new structure of molecular sieves and extend the application of molecular sieves as well.

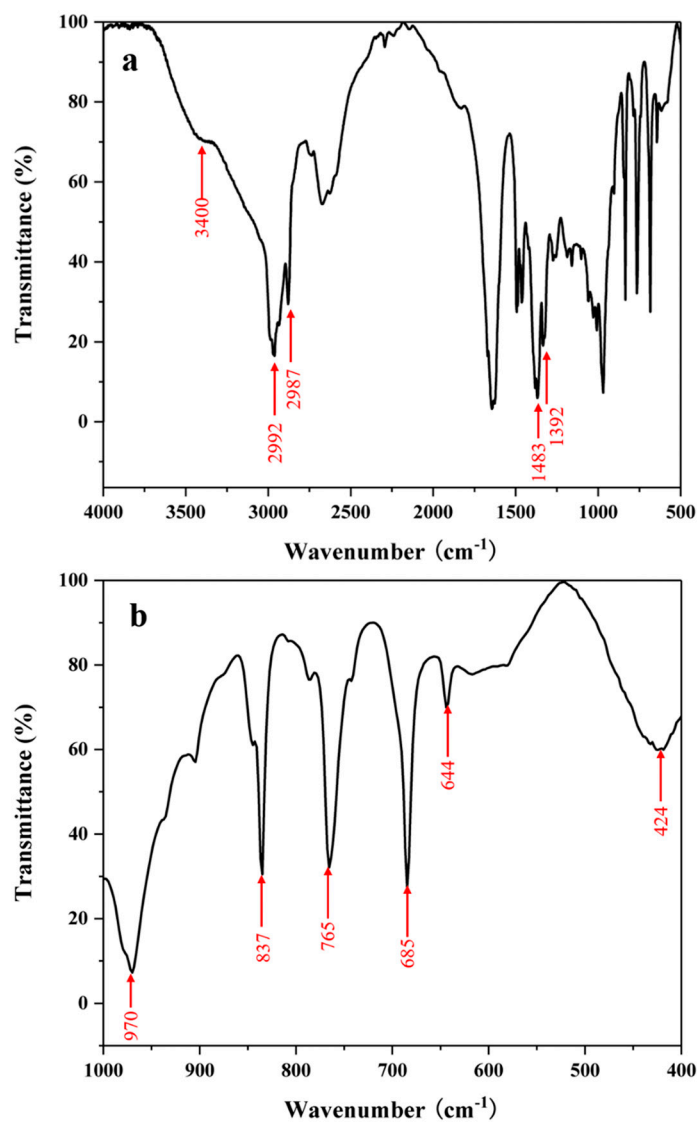


**Figure 9.** FTIR spectrum of BUCT-3: (a) Full FTIR spectrum (b) fingerprint region spectrum.

**Table 5.** Element analysis of BUCT-3.

Element	Weight Percentage (%)				Atom Ratio
	N	C	H	O	C/N
BUCT-3	4.62	50.94	9.88	34.56	12.86

The full spectrum XPS of BUCT-3 and the high-resolution XPS of O are shown in Figure 10. From the full spectrum, we can see the main elements such as Si, Al, O, C, and N in the template. From the peak fitting spectrum of O, it can be known that in addition to the skeleton O with binding energy at 532 eV and the surface silanol  $\text{OH}^-$  at 531 eV, there is a most typical  $\text{O}_2^{2-}$  peak at 530 eV. Through quantitative analysis and calculation, we have obtained 6.4%  $\text{O}_2^{2-}$  of the total O 1s. Since BUCT-3 is prepared from SiAl-2, only a small part of the 23% oxygen in SiAl-2 enters the final structure. This is because most of the O-O is decomposed by heating during the crystallization process. Combined with the above infrared analysis, the conclusion that the peroxide bonds in the aluminosilica perhydrate hydrogel are retained in the framework of the product has been strongly proved.

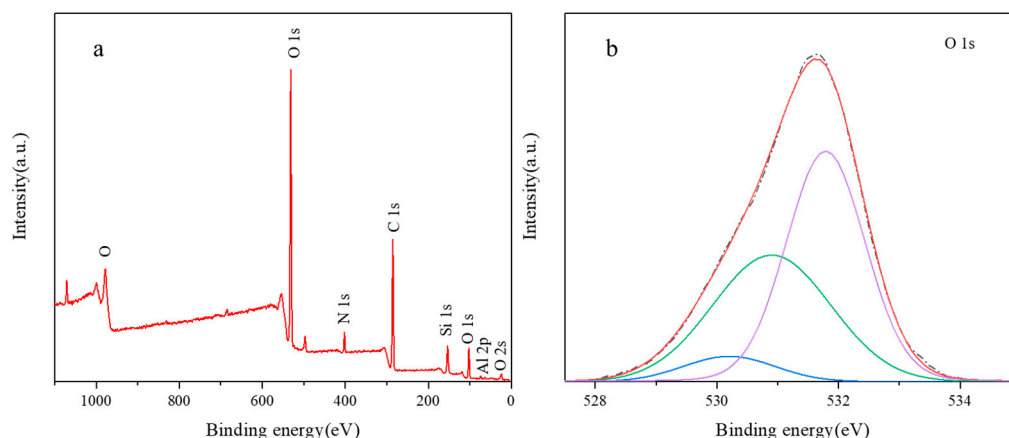


**Figure 10.** XPS spectra of BUCT-3: (a) the full XPS survey spectra, (b) high-resolution XPS spectra of O.

In situ variable temperature XRD analysis reveals the thermostability of the as-synthesized BUCT-3 (Figure 11). BUCT-3 molecular sieves started to collapse at 140 °C, which can be clearly seen from the significant decrease of the peaks' intensities. It is probably because the O-O bonds in the framework of BUCT-3 broke during the heating process. Hence, the optimal calcination condition for BUCT-3 to remove templates is at a lower temperature, like 120 °C, in the presence of ozone and this work is still in progress.

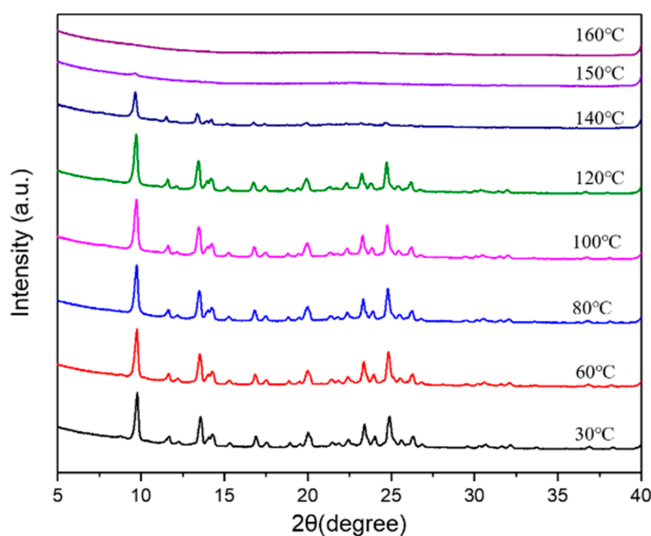


**Figure 11.** In situ variable temperature XRD patterns of BUCT-3.

Based on the above conclusions and the hydrogen-bond induced crystallization mechanism of zeolites [40], we can reasonably speculate on the crystallization process of zeolites with the new structure. In the early stage of the reaction, aluminosilica perhydrate hydrogel first depolymerizes into a large number of monomeric and dimeric species with hydrogen-bond (H-O-O). Then, these species condense around TPA+ through the hydrogen bonds on its surface. These hydrogen bonds from the  $[(\text{HO})_3\text{SiOSi}(\text{OH})_3]\text{-H}_2\text{O}_2$  [31] or  $\text{SiO}^- \cdots \text{HO-Si}$  [40] serve as the connectors to bridge the silicates together and fuse themselves to form the long-range periodic framework. During the condensation process, the peroxide bond (O-O) of hydrogen peroxide is finally incorporated into the framework.

#### 4. Conclusions

In this paper, two kinds of new silicon and aluminum sources obtained by gel-sol method are aluminosilica perhydrate hydrogels and both of them have amorphous phase with nano-sphere morphology. FTIR analysis was used to confirm the existence of O-O bonds in the silicon and aluminum source, SiAl-1 and SiAl-2. Pure phase molecular sieves, BUCT-3, was hydrothermally synthesized by using TPAOH as SDA under mild reacting condition. The key to synthesize this new aluminosilicate is using aluminosilica perhydrate hydrogel with relatively high O-O bond contents, SiAl-2, as the silicon and aluminum source. The cell parameters of BUCT-3 determined by XRD were  $a = 8.9645 \text{ \AA}$ ,  $b = 15.2727 \text{ \AA}$ ,  $c = 11.3907 \text{ \AA}$ ,  $\alpha = 90^\circ$ ,  $\beta = 93.858^\circ$ ,  $\gamma = 90^\circ$ . Since the O-O bonds remained in the structure of BUCT-3, its thermostability is not good. Despite the advances described in the structure elucidation of new materials, there are occasions where the achievement of the real structure of unstable materials is still a complex problem. Therefore, it is necessary to develop a new characterization technique or preparation procedure to solve this extremely unstable structure, so that the detailed structure information of the molecular sieve with peroxide bond in the framework can be obtained. Nevertheless, BUCT-3 molecular sieves may have potential application as a bleaching and oxidizing agent. Besides, this new synthesis method of  $\text{H}_2\text{O}_2$  treatment provides an effective strategy for the design of new molecular sieves.

**Supplementary Materials:** The following are available online at <http://www.mdpi.com/1996-1944/13/23/5469/s1>, Figure S1: the selected area electron diffraction (SAED) of BUCT-3: (a) Irradiate for 1 minute (b) Irradiate for 2 minutes (c) Irradiate for 2.5 minutes.

**Author Contributions:** Conceptualization, K.J.; Formal analysis, H.M.; Investigation, H.M. and K.J.; Methodology, H.M.; Supervision, X.X. and J.S.; Writing—original draft, H.M. and K.J.; Writing—review & editing, X.X. and J.S. All authors have read and agreed to the published version of the manuscript.

**Funding:** This research was funded by [The Shanghai Key Laboratory of Green Chemistry and Chemical Processes] grant number [H2016107].

**Conflicts of Interest:** The authors declare no conflict of interest.

#### References

1. Rabo, J.A.; Kasai, P.H. Caging and electrolytic phenomena in zeolites. *Prog. Solid State Chem.* **1975**, *9*, 1–19. [[CrossRef](#)]
2. Barthomeuf, D.A. General hypothesis on zeolites physicochemical properties. Applications to adsorption, acidity, catalysis, and electrochemistry. *J. Phys. Chem.* **1979**, *83*, 249–256. [[CrossRef](#)]
3. Corma, A.; Davis, M.E. Issues in the synthesis of crystalline molecular sieves: Towards the crystallization of low framework-density structures. *Chem. Phys. Chem.* **2004**, *5*, 304–313. [[CrossRef](#)] [[PubMed](#)]
4. Zones, S.I. Translating new materials discoveries in zeolite research to commercial manufacture. *Microporous Mesoporous Mater.* **2011**, *144*, 1–8. [[CrossRef](#)]
5. Li, J.; Corma, A.; Yu, J. Synthesis of new zeolite structures. *Chem. Soc. Rev.* **2015**, *44*, 7112–7127. [[CrossRef](#)] [[PubMed](#)]
6. Moliner, M.; Rey, F.; Corma, A. Towards the rational design of efficient organic structure-directing agents for zeolite synthesis. *Angew. Chemie Int. Ed.* **2013**, *52*, 13880–13889. [[CrossRef](#)] [[PubMed](#)]

7. Goepper, M.; Li, H.-X.; Davis, M.E. A possible role of alkali metal ions in the synthesis of pure-silica molecular sieves. *J. Chem. Soc. Chem. Commun.* **1992**, *22*, 1665–1666. [[CrossRef](#)]
8. Li, J.; Yu, J.; Xu, R. Progress in heteroatom-containing aluminophosphate molecular sieves. *Proc. R. Soc. A Math. Phys. Eng. Sci.* **2012**, *468*, 1955–1967. [[CrossRef](#)]
9. Yi, T.; Xu, J.; Zi, G. Isomorphous substitution of metallic elements for zeolite Y in the aqueous solution. *Chem. Res. Chin. Univ.* **1990**, *4*, 332–340.
10. Xu, Z.L.; Zhang, Y.Z.; Zheng, L.B. The secondary synthesis of zeolites via framework substitution for aluminum I preparation and characterization of zeolite Y containing Ga. *J. Mol. Catal.* **1992**, *6*, 271–278.
11. Dwyer, J.; Karim, K. The incorporation of heteroatoms into faujastic framework by secondary synthesis using aqueous fluoride complexes. *J. Chem. Soc. Chem. Commun.* **1991**, *14*, 905–906. [[CrossRef](#)]
12. Roth, W.J.; Nachtigall, P.; Morris, R.E.; Cejka, J. Two-dimensional zeolites: Current status and perspectives. *Chem. Rev.* **2014**, *114*, 4807–4837. [[CrossRef](#)] [[PubMed](#)]
13. Diaz, U.; Corma, A. Layered zeolitic materials: An approach to designing versatile functional solids. *Dalton Trans.* **2014**, *43*, 10292–10316. [[CrossRef](#)] [[PubMed](#)]
14. Auerbach, S.M.; Carrado, K.A.; Dutta, P.K. *Handbook of Zeolite Science and Technology*; CRC press: Boca Raton, FL, USA, 2003.
15. Dai, F.Y.; Suzuki, M.; Takahashi, H.; Saito, Y. *Zeolite Synthesis*; Occelli, M.L., Robson, H.E., Eds.; American Chemical Society: Washington, DC, USA, 1989.
16. Ryozi, H.; Yoshiro, M. Effects of changes of mother-liquor composition on crystallization process. *Mem. Fac. Sci. Shimane Univ.* **1994**, *28*, 47–58.
17. Warzywoda, J.; Dixon, A.G.; Thompson, R.W.; Sacco Jr, A.; Suib, S.L. The role of the dissolution of silicic acid powders in aluminosilicate synthesis mixtures in the crystallization of large mordenite crystals. *Zeolites* **1996**, *16*, 125–137. [[CrossRef](#)]
18. Warzywoda, J.; Dixon, A.G.; Thompson, R.W.; Sacco, A. Synthesis and control of the size of large mordenite crystals using porous silica substrates. *J. Mater. Chem.* **1995**, *5*, 1019–1025. [[CrossRef](#)]
19. Zhu, G.; Qiu, S.; Yu, J.; Gao, F.; Xiao, F.; Xu, R.; Sakamoto, Y.; Terasaki, O. *Synthesis of Zeolite LTA Single Crystals of Macro-to Nanometer Size*; Materials Research Society: Warrendale, PA, USA, 1999; pp. 1863–1870.
20. Kalipcilar, H.; Culfaz, A. Influence of nature of silica source on template-free synthesis of ZSM-5. *Cryst. Res. Technol. J. Exp. Ind. Crystallogr.* **2001**, *36*, 1197–1207. [[CrossRef](#)]
21. Kalipcilar, H.; Culfaz, A. Synthesis of submicron silicalite-1 crystals from clear solutions. *Cryst. Res. Technol. J. Exp. Ind. Crystallogr.* **2000**, *35*, 933–942. [[CrossRef](#)]
22. Li, Q.; Mihailova, B.; Creaser, D.; Sterte, J. Aging effects on the nucleation and crystallization kinetics of colloidal TPA-silicalite-1. *Microporous Mesoporous Mater.* **2001**, *43*, 51–59. [[CrossRef](#)]
23. Ko, Y.S.; Chang, S.H.; Ahn, W.S. 02-P-19-effects of synthesis parameters on zeolite I crystallization. *Stud. Surf. Sci. Catal.* **2001**, *135*, 189.
24. Schmidt, W.; Toktarev, A.V.; Schueth, F.; Ione, K.G.; Unger, K. 02-P-23-the influence of different silica sources on the crystallization kinetics of zeolite beta. *Stud. Surf. Sci. Catal.* **2001**, *135*, 190.
25. Hamidi, F.; Pamba, M.; Bengueddach, A.; Di Renzo, F.; Fajula, F. 03-P-19-factors affecting composition and morphology of mordenite. *Stud. Surf. Sci. Catal.* **2001**, *135*, 334.
26. Lowe, B.M.; MacGilp, N.A.; Whittam, T.V. Active silicates and their role in zeolite synthesis. In Proceedings of the 5th International Conference on Zeolites, Naples, Italy, 2–6 June 1980.
27. Rabo, J.A.; Schoonover, M.W. Early discoveries in zeolite chemistry and catalysis at union carbide, and follow-up in industrial catalysis. *Appl. Catal. A Gen.* **2001**, *222*, 261–275. [[CrossRef](#)]
28. Mohamed, R.M.; Aly, H.M.; El-shahat, M.F.; Ibrahim, I.A. Effect of the silica sources on the crystallinity of nanosized ZSM-5 zeolite. *Microporous Mesoporous Mater.* **2005**, *79*, 7–12. [[CrossRef](#)]
29. Elkin, P.B.; Shull, C.G.; Roess, L.C. Silica-alumina, gels. *Ind. Eng. Chem.* **1945**, *37*, 327–331. [[CrossRef](#)]
30. Plank, C.J.; Drake, L.C. Differences between silica and silica-alumina gels. Factors affecting the porous structure of these gels. *J. Colloid Sci.* **1947**, *2*, 399–412. [[CrossRef](#)]
31. Zegliński, J.; Piotrowski, G.P.; Piekoś, R. A study of interaction between hydrogen peroxide and silica gel by FTIR spectroscopy and quantum chemistry. *J. Mol. Struct.* **2006**, *794*, 83–91. [[CrossRef](#)]
32. Wolanov, Y.; Shurki, A.; Prikhodchenko, P.V.; Tripol'skaya, T.A.; Novotortsev, V.M.; Pedahzur, R.; Lev, O. Aqueous stability of alumina and silica perhydrate hydrogels: Experiments and computations. *Dalton Trans.* **2014**, *43*, 16614–16625. [[CrossRef](#)]

33. Szulbinski, W.S. ESR and resonance raman spectroscopic studies of peroxide intermediates derived from iron diazaoxacyclononane. *Spectrochim. Acta Part A Mol. Biomol. Spectrosc.* **2000**, *56*, 2117–2124. [[CrossRef](#)]
34. Prabhakaran, K.; Rao, C.N.R. A Combined Eels-Xps study of molecularly chemisorbed oxygen on silver surfaces: Evidence for superoxo and peroxy species. *Surf. Sci.* **1987**, *186*, 575–580. [[CrossRef](#)]
35. Scholes, F.H.; Hughes, A.E.; Hardin, S.G.; Lynch, P.; Miller, P.R. Influence of hydrogen peroxide in the preparation of nanocrystalline ceria. *Chem. Mater.* **2007**, *19*, 2321–2328. [[CrossRef](#)]
36. Scholle, K.F.M.G.J.; Veeman, W.S.; Frenken, P.; Velden, G.P.M.V.D. Characterization of intermediate TPA-ZSM-5 type structures during crystallization. *Appl. Catal.* **1985**, *17*, 233–259. [[CrossRef](#)]
37. Koningsveld, H.V.; Bekkum, H.V.; Jansen, J.C. On the location and disorder of the tetrapropylammonium (TPA) ion in zeolite ZSM-5 with improved framework accuracy. *Acta Crystallogr.* **1987**, *43*, 127–132. [[CrossRef](#)]
38. Database of Zeolite Structures. Available online: [https://asia.iza-structure.org/IZA-SC/pow\\_pat\\_user-data.php](https://asia.iza-structure.org/IZA-SC/pow_pat_user-data.php) (accessed on 15 May 2018).
39. Flanigen, E.M.; Khatami, H.; Szymanski, H.A. Infrared Structural Studies of Zeolite Frameworks. In *Molecular Sieve Zeolites; Advances in Chemistry*; Washington, DC, USA, 1971; pp. 201–229.
40. Liu, X.; Wang, Q.; Wang, C.; Xu, J.; Deng, F. Hydrogen-bond induced crystallization of silicalite-1 zeolite as revealed by solid-state NMR spectroscopy silicalite-1. *Acta Phys. Sin.* **2020**, *36*, 1–9.

**Publisher's Note:** MDPI stays neutral with regard to jurisdictional claims in published maps and institutional affiliations.



© 2020 by the authors. Licensee MDPI, Basel, Switzerland. This article is an open access article distributed under the terms and conditions of the Creative Commons Attribution (CC BY) license (<http://creativecommons.org/licenses/by/4.0/>).